Constitutive Immune Activity Promotes Tumorigenesis in *Drosophila* Intestinal Progenitor Cells.

Kristina Petkau, Meghan Ferguson, Silvia Guntermann, Edan Foley*.

Department of Medical Microbiology and Immunology

Institute of Virology

University of Alberta

Edmonton, Alberta

Canada.

*Corresponding author.

Email: efoley@ualberta.ca

SUMMARY

Gut innate immune defenses contain bacterial populations and protect the host interior from invasive microbes. Although excess intestinal immune activity frequently promotes inflammatory illnesses, we know little about the consequences of chronic innate immune activity exclusively in endodermal gut cells of an otherwise normal animal. To address this question, we generated a transgenic line that allows us to activate inflammatory signals in adult fly intestinal progenitor cells. We found that constitutive immune activity in intestinal progenitors disrupts expression of homeostatic regulators such as Notch signal transduction pathway components and induces hyperplasia throughout the gut. Consistent with these observations, we found that persistent immune signaling interferes with progenitor cell differentiation and exacerbates the formation of Notch-dependent intestinal tumors. These findings uncover a novel link between constitutive immune activity and tumorigenesis in intestinal stem cells.

28 **INTRODUCTION**

29

30 The endoderm is at the heart of an ancient, intimate, and continuous relationship between
31 multicellular organisms and the microbial world. Gut commensals negotiate a semi-stable
32 existence within host niches, partially through provision of factors that influence nutrition,
33 development, and immunity in the host (Cho and Blaser, 2012). For their part, hosts invest energy
34 and resources in the containment of intestinal microbes (Hooper et al., 2012). Physical barriers
35 such as the peritrophic matrix of insects, or dense mucosal layers of mammals, keep microbes at
36 an adequate distance from gut cells. Additionally, host-derived reactive oxygen and nitrogen
37 species destroy invading microbes, while antimicrobial effectors block microbial dissemination.
38 The consequences of failed antibacterial defenses are often extreme, and occasionally deadly for
39 the host. For example, dysbiotic microbial communities contribute to traumatic inflammatory
40 bowel diseases in humans (Wlodarska et al., 2015). In recent years, we have made considerable
41 advances in understanding relationships between host immune responses and gut microbiota
42 (Honda and Littman, 2016). Germline-encoded innate immune systems provide critical defenses
43 in the endoderm, a primary site of contact between multicellular organisms and their immediate
44 microbial environment. Thus, characterization of innate immune regulation in endodermal
45 tissues is essential for a full appreciation of the mechanistic basis for the restraint of gut microbes.
46 The fruit fly, *Drosophila melanogaster*, is widely used for the characterization of intestinal
47 development and function (Buchon et al., 2013, Jiang and Edgar, 2012, Lemaitre and Miguel-
48 Aliaga, 2013). For example, *Drosophila* is an excellent model for the exploration of Notch-
49 mediated regulation of gut development (Guo and Ohlstein, 2015, Micchelli and Perrimon, 2006,

50 Ohlstein and Spradling, 2006, Ohlstein and Spradling, 2007), and intestinal tumorigenesis (Patel
51 and Edgar, 2014, Biteau and Jasper, 2011, Marianes and Spradling, 2013, Apidianakis et al., 2009).
52 In the fly midgut, basal intestinal stem cells (ISC) divide to generate a bipotent transient cell type,
53 the enteroblast (EB). Delta-Notch signals between ISC-EB progenitor pairs determine the
54 developmental fate of EBs (Takashima et al., 2011, Perdigoto et al., 2011). High levels of Notch
55 activity in enteroblasts lead to their differentiation as large, polyploid, absorptive enterocytes
56 (EC). Lower levels of Notch activity result in the differentiation of enteroblasts as smaller, diploid,
57 secretory enteroendocrine cells (EE). Notch-dependent control of progenitor cell differentiation
58 is conserved across vast evolutionary distances, with similar requirements in species as diverse
59 as fish and rodents (Fre et al., 2005, Stanger et al., 2005, van Es et al., 2005, Crosnier et al., 2005),
60 and interruptions to Notch signaling lead to intestinal tumor formation in several models
61 (Kazanjian and Shroyer, 2011, Peignon et al., 2011).
62 Current data implicate the immune deficiency (IMD) pathway as a central regulator of
63 antibacterial defenses in the fly gut (Buchon et al., 2009, Lhocine et al., 2008). IMD shares
64 numerous features with the mammalian tumor necrosis factor (TNF) cascade (Buchon et al.,
65 2014). In the fly, detection of bacterial peptidoglycan results in the proteolytic removal of thirty
66 N-terminal amino acids from the Imd adaptor protein by the caspase Dredd (Paquette et al.,
67 2010). Cleaved Imd associates with the Inhibitor of Apoptosis 2 (IAP2) and Fas-Associated Death
68 Domain (FADD) orthologs (Guntermann and Foley, 2011, Paquette et al., 2010) to activate the
69 NF-kB transcription factor Relish (Dushay et al., 1996). Active Relish relocates to the nucleus and
70 initiates transcription of a broad spectrum of antimicrobial peptides. More recent work showed
71 that intestinal IMD activity also controls the expression of genes involved in developmental and

72 metabolic processes (Broderick et al., 2014, Erkosar et al., 2014). These studies hint at novel,
73 unstudied biological roles for IMD that extend beyond the extermination of unwanted bacteria.
74 Here, we characterized the consequences of persistent IMD activity in midgut progenitors.
75 Midgut progenitor cells extend projections into the intestinal lumen (Ohlstein and Spradling,
76 2006), and express IMD pathway genes at levels comparable to mature epithelial cells (Dutta et
77 al., 2015). In addition, enteric challenges with bacterial pathogens induce classic IMD-response
78 genes in progenitor cells (Dutta et al., 2015, Fink et al., 2016), confirming progenitor cells as an
79 immune-competent compartment. However, the effects of IMD activity on progenitor cells is
80 unclear. To address this, we engineered a novel IMD variant that permits temporal and cell-
81 specific activation of IMD. We showed that constitutive immune signaling altered the expression
82 of Notch pathway regulators, disturbed EE differentiation, and caused hyperplasia throughout
83 the posterior midgut. Consistent with interactions between IMD and Notch, we found that
84 constitutive IMD activity greatly exacerbated the formation of Notch-dependent tumors. Given
85 the involvement of inflammation and Notch signaling in vertebrate intestinal tumor
86 development, we believe our findings may be relevant to studies that explore relationships
87 between intestinal inflammation and tumorigenesis.
88

89 **RESULTS**

90 *Constitutive IMD Pathway Activation in Intestinal Stem Cells.*

91 To characterize the effects of constitutive immune signaling in the intestine, we generated a
92 transgenic *Drosophila* line that allows cell-restricted activation of the IMD pathway. Specifically,
93 we engineered a truncated IMD protein that uses an internal ATG (at residue 78) as a start codon.
94 We refer to this truncated protein as ImdCA. ImdCA lacks inhibitory N-terminal amino acids
95 (Figure 1A), but retains the ability to interact with the FADD adaptor protein (Figure 1B). We
96 generated transgenic fly lines that permit temperature-dependent expression of ImdCA in fat
97 tissue (*cgGAL4* ; *GAL80^{ts}/UASimdCA* (abbreviated as *cg^{ts}>CA*)), or ISC/EB progenitor cell pairs
98 (*esgGAL4*, *GAL80^{ts}*, *UASGFP* ; *UASimdCA* (abbreviated as *esg^{ts}>CA*)). Incubation of either
99 genotype at 29°C, the restrictive temperature for *GAL80^{ts}*, results in tissue-specific expression of
100 ImdCA in fat body or intestinal progenitor cells, respectively. In the fat body, the principle site of
101 humoral immunity, ImdCA caused expression of the IMD-responsive antimicrobial peptides *dpt*
102 and *att* (Figure 1C). The induction of *dpt* and *att* proceeded via a classical IMD response, as null
103 mutations in *dredd* prevented ImdCA-mediated antimicrobial peptide expression (Figure 1D).
104 ImdCA is equally effective at inducing antimicrobial expression in midgut progenitor cells (Figure
105 1E), and expression of ImdCA provided protective benefits against lethal challenges with the
106 gastrointestinal pathogen *Vibrio cholerae* (Figure 1F). These data show that we have established
107 a novel fly line that permits tissue-specific activation of IMD responses in *Drosophila*.

108

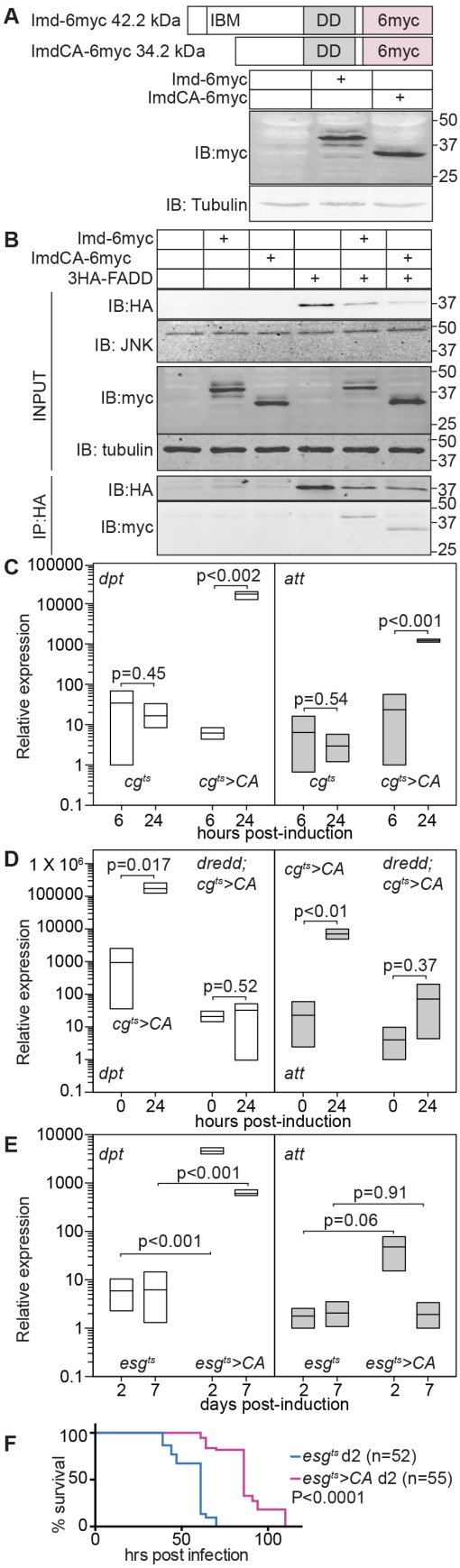
A
Imd-6myc 42.2 kDa
IBM
DD
6myc
ImdCA-6myc 34.2 kDa
DD
6myc
Imd-6myc
ImdCA-6myc
IB:myc
IB: Tubulin
50
37
25
B
Imd-6myc
ImdCA-6myc
3HA-FADD
INPUT
IB:HA
IB: JNK
IB:myc
IB: tubulin
IP:HA
IB:HA
IB:myc
C
Relative expression
dpt
att
p<0.002
p<0.001
p=0.45
p=0.54
cg^ts
cg^ts>CA
hours post-induction
D
p=0.017
dredd; cg^ts>CA
p<0.01
p=0.37
p=0.52
hours post-induction
E
p<0.001
p=0.91
p=0.06
esg^ts
esg^ts>CA
days post-induction
F
% survival
esg^ts d2 (n=52)
esg^ts>CA d2 (n=55)
P<0.0001
hrs post infection

FIGURE 1

109

110 **Figure 1. A truncated Imd protein activates innate immune responses. (A)** Schematic
111 representation of C-terminally myc-tagged Imd and ImdCA. Iap Binding Motif (IBM) and death
112 domain (DD) are indicated. Western blots show lysates of untransfected S2 cells (lane 1) S2 cells
113 transfected with expression constructs for Imd-6myc (lane 2), and ImdCA-6myc (lane 3). Numbers
114 indicated molecular weights in kDa. The membrane was probed with Tubulin as a loading control.
115 **(B)** S2 cells were transfected with the indicated expression constructs and input samples (blots
116 labeled INPUT) were probed for the indicated antigens. Anti-HA immunoprecipitates (blots
117 labeled IP:HA) were probed with the indicated antibodies. **(C-E)** Quantification of the relative
118 expression levels of *dpt* and *att* in flies raised at 29°C for the indicated time. Survival curves of
119 *esg^{ts}>CA* and *esg^{ts}* flies raised at 29°C for two days, and then challenged with *Vibrio cholerae*.
120
121 *A Balance of Microbial Cues and Host Immune Status Determines Gene Expression Patterns in the*
122 *Adult Midgut*.
123 Intestinal progenitor cells express IMD pathway components at similar levels to epithelial cell
124 (Figure 5A), and display classical IMD-responses to microbial challenges (Dutta et al., 2015). To
125 characterize the effects of ImdCA expression in intestinal progenitors, we prepared
126 transcriptional profiles of the intestines of *esg^{ts}* and *esg^{ts}>CA* adult flies that we raised at 18°C for
127 ten days, and shifted to 29°C for two days. We examined *esg^{ts}* and *esg^{ts}>CA* flies raised under
128 conventional or germ-free conditions in these studies. This strategy allowed us to make pairwise
129 comparisons of the effects of commensal bacteria and ImdCA on the control of host transcription
130 (Figure 2A-D).
131

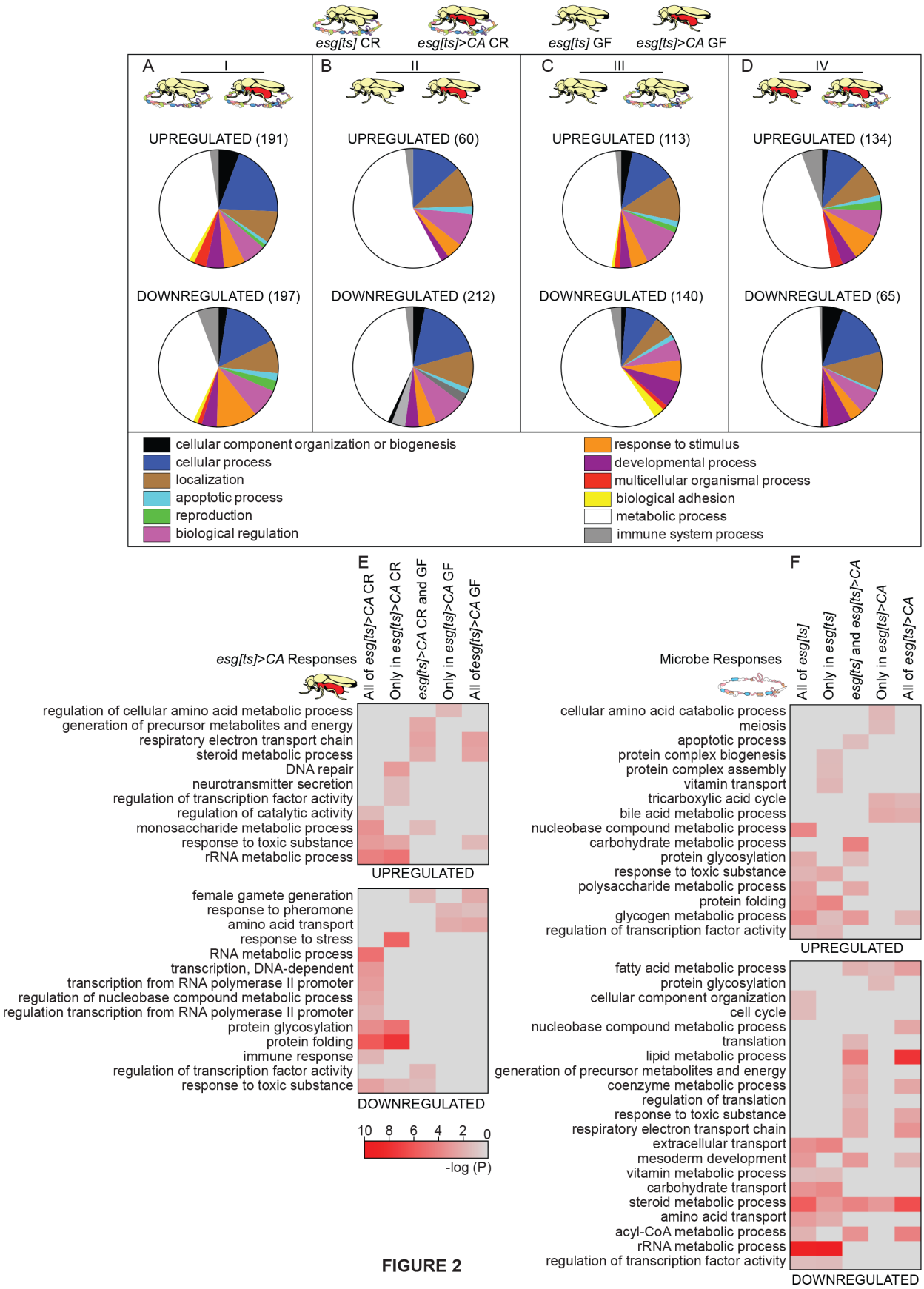
esg[ts] CR
esg[ts]>CA CR
esg[ts] GF
esg[ts]>CA GF
A
I
UPREGULATED (191)
DOWNREGULATED (197)
B
II
UPREGULATED (60)
DOWNREGULATED (212)
C
III
UPREGULATED (113)
DOWNREGULATED (140)
D
IV
UPREGULATED (134)
DOWNREGULATED (65)
cellular component organization or biogenesis
cellular process
localization
apoptotic process
reproduction
biological regulation
response to stimulus
developmental process
multicellular organismal process
biological adhesion
metabolic process
immune system process
E
esg[ts]>CA Responses
All of esg[ts]>CA CR
Only in esg[ts]>CA CR
esg[ts]>CA CR and GF
Only in esg[ts]>CA GF
All ofesg[ts]>CA GF
regulation of cellular amino acid metabolic process
generation of precursor metabolites and energy
respiratory electron transport chain
steroid metabolic process
DNA repair
neurotransmitter secretion
regulation of transcription factor activity
regulation of catalytic activity
monosaccharide metabolic process
response to toxic substance
rRNA metabolic process
UPREGULATED
female gamete generation
response to pheromone
amino acid transport
response to stress
RNA metabolic process
transcription, DNA-dependent
transcription from RNA polymerase II promoter
regulation of nucleobase compound metabolic process
regulation transcription from RNA polymerase II promoter
protein glycosylation
protein folding
immune response
regulation of transcription factor activity
response to toxic substance
DOWNREGULATED
10 8 6 4 2 0
-log (P)
F
Microbe Responses
All of esg[ts]
Only in esg[ts]
esg[ts] and esg[ts]>CA
Only in esg[ts]>CA
All of esg[ts]>CA
cellular amino acid catabolic process
meiosis
apoptotic process
protein complex biogenesis
protein complex assembly
vitamin transport
tricarboxylic acid cycle
bile acid metabolic process
nucleobase compound metabolic process
carbohydrate metabolic process
protein glycosylation
response to toxic substance
polysaccharide metabolic process
protein folding
glycogen metabolic process
regulation of transcription factor activity
UPREGULATED
fatty acid metabolic process
protein glycosylation
cellular component organization
cell cycle
nucleobase compound metabolic process
translation
lipid metabolic process
generation of precursor metabolites and energy
coenzyme metabolic process
regulation of translation
response to toxic substance
respiratory electron transport chain
extracellular transport
mesoderm development
vitamin metabolic process
carbohydrate transport
steroid metabolic process
amino acid transport
acyl-CoA metabolic process
rRNA metabolic process
regulation of transcription factor activity
DOWNREGULATED

132

FIGURE 2

133 **Figure 2. ImdCA and the microbiome interact to control gut transcription. A-B:** Graphic
134 representation of biological functions dysregulated in *esg*^{ts}*>CA* flies relative to *esg*^{ts} flies raised
135 under conventional (A) or germ-free conditions (B). **C-D:** Graphic representation of biological
136 functions dysregulated in conventional flies relative to germ-free flies in the absence (C) or
137 presence (D) of ImdCA expression. For A-D, numbers indicated total numbers of dysregulated
138 genes. Genes with unknown function were not included in pie charts. **(E-F)** Heatmap of
139 significance scores for gene ontology terms (minimum 5 genes in each term) that were
140 significantly dysregulated in *esg*^{ts}*>CA* flies relative to *esg*^{ts} flies (E), or conventionally-reared
141 relative to germ-free flies (F). In E, GO terms are further subdivided into terms that were
142 dysregulated in conventionally-reared or germ-free flies. In F, GO terms are subdivided into terms
143 that were dysregulated in *esg*^{ts} flies and *esg*^{ts}*>CA* flies.
144
145 Similar to earlier studies (Broderick et al., 2014, Erkosar et al., 2014), we found that the
146 microbiome regulates the expression a large cohort of host genes, with a particularly notable
147 effect on genes involved in metabolic processes (Figure 2A-D, Figure 3). As expected, ImdCA
148 altered the expression of genes with known roles in innate defenses. However, we also noticed
149 effects of ImdCA on pathways as diverse as metabolism, transportation and stress responses
150 (Figures 2, 3).
151 Comparisons between the individual expression profiles uncovered substantial effects of the
152 microbiome on ImdCA-regulated transcription. For example, only 35 host genes are induced in
153 both conventionally-reared and germ-free animals in response to ImdCA (Figure 3E). In contrast,
154 146 transcripts are only induced in the presence of an intact microbiome, and an additional 21

155 transcripts are only induced in the absence of a microbiome (Figure 3E). Likewise, microbiome-
156 response genes are heavily influenced by the extent of immune activity in the gut. For example,
157 a unique set of 129 genes responds to presence of the microbiome only upon induction of ImdCA
158 (Figure 3F). GO term analysis showed that the microbiome and immune activity synergistically
159 influence functional outputs in the gut. For example, ImdCA only promotes protein glycosylation
160 in the presence of a microbiome (Figure 2E), and the gut microbiome induces tricarboxylic acid
161 cycle genes only when accompanied by intestinal inflammation (Figure 2F). Combined, these data
162 show that gut transcriptional outputs reflect the extent of immune activity and microbial
163 presence in the gut.
164

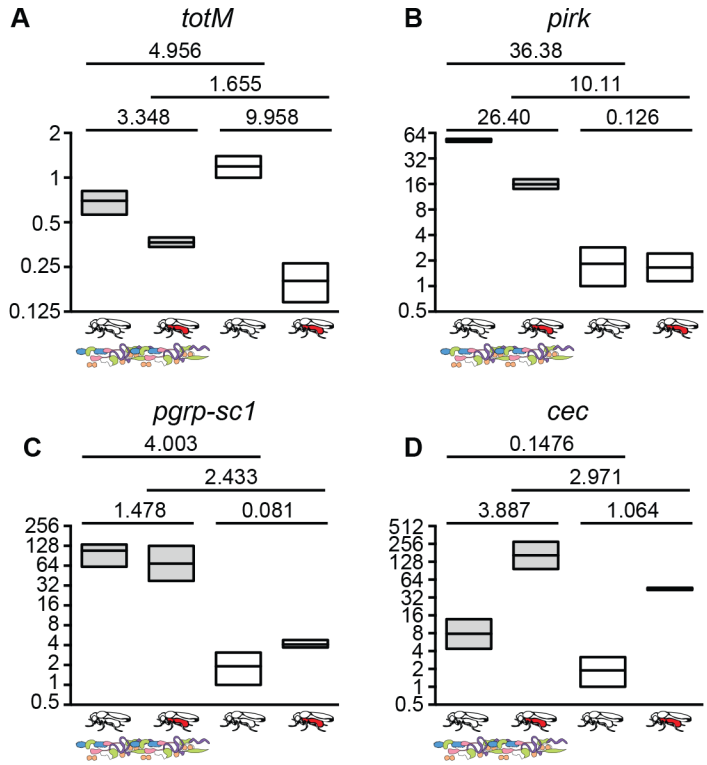

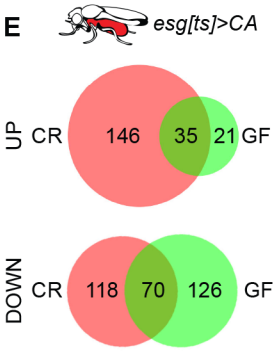

esg[ts]>CA response.	CR	GF
IMMUNE RESPONSE	16	11
SIGNAL TRANSDUCTION	38	12
MAINTENANCE OF STEM CELL IDENTITY	4	
DEVELOPMENT	9	
METABOLISM	63	31
TRANSPORT	21	19
OXIDATION-REDUCTION	17	11
ION HOMEOSTASIS	5	5
STRESS RESPONSE	26	10
OTHER	19	20
CHITIN BINDING		8
STEROL INTERACTING		6

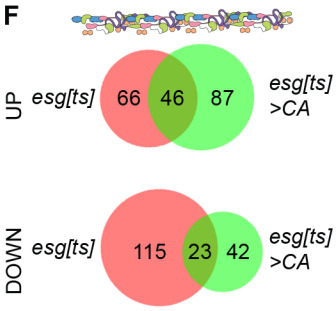

Microbiome response.	*esg[ts]*	*esg[ts] >CA*
IMMUNE RESPONSE	15	11
SIGNAL TRANSDUCTION	15	11
METABOLISM	58	40
TRANSPORT	23	11
OXIDATION-REDUCTION	11	11
ION HOMEOSTASIS		4
STRESS RESPONSE	16	5
OTHER	26	19
CHITIN BINDING	8	
STEROL INTERACTING		5

Figure 3: A-D: Relative expression of totM (A), pirk (B), pgrp-sc1 (C) and cec (D) in the dissected

168 intestines of conventionally-reared or germ-free *esg*^{ts} flies or *esg*^{ts}*>CA* flies. For each assay,
169 expression levels were reported relative to those observed in germ-free *esg*^{ts} flies. Comparisons
170 were performed with a Sidak's multiple comparison test. Values show the Sidak's t value for the
171 respective tests. **E:** Number of genes and GO terms that were up or downregulated in *esg*^{ts}*>CA*
172 flies relative to *esg*^{ts} flies raised under conventional (CR) or germ-free (GF) conditions. **F:** Number
173 of genes and GO terms that were up or downregulated in conventionally-reared flies relative to
174 germ-free flies of the indicated genotypes.
175
176 Given the effects of ImdCA on antimicrobial peptide expression, we assumed that ImdCA will
177 affect composition of the host microbiome. To test this, we treated freshly eclosed *esg*^{ts} and
178 *esg*^{ts}*>CA* flies with a regime of antibiotics for six days to eliminate the endogenous microbiome.
179 We then fed all flies a homogenate prepared from our lab wild-type *Drosophila* strain, and
180 passaged flies to fresh food twice over seven days to facilitate stable association between
181 microbes in the homogenate and the recipient flies. After seven days, we shifted recipients to
182 29°C for an additional seven days to activate the IMD pathway in *esg*^{ts}*>CA* flies. We dissected the
183 intestines of the different populations and used deep-sequencing of 16S DNA to identify the
184 bacterial communities present in the respective guts (Figure 4). As expected, the bacterial
185 microbiome of *esg*^{ts} flies was barely distinguishable from the homogenate. Both microbiomes
186 contained a limited number of OTUs characterized primarily by *Acetobacter* and *Lactobacilli*
187 (Figure 4). Contrary to our initial expectation, we did not observe a significant impact of ImdCA
188 on microbiome composition. In fact, the bacterial communities of the original homogenate, the

189 *esg*^{ts} flies, and the *esg*^{ts}*>CA* flies were barely distinguishable (Figure 4), suggesting that acute

190 activation of IMD does not significantly alter microbial populations in the gut.

191

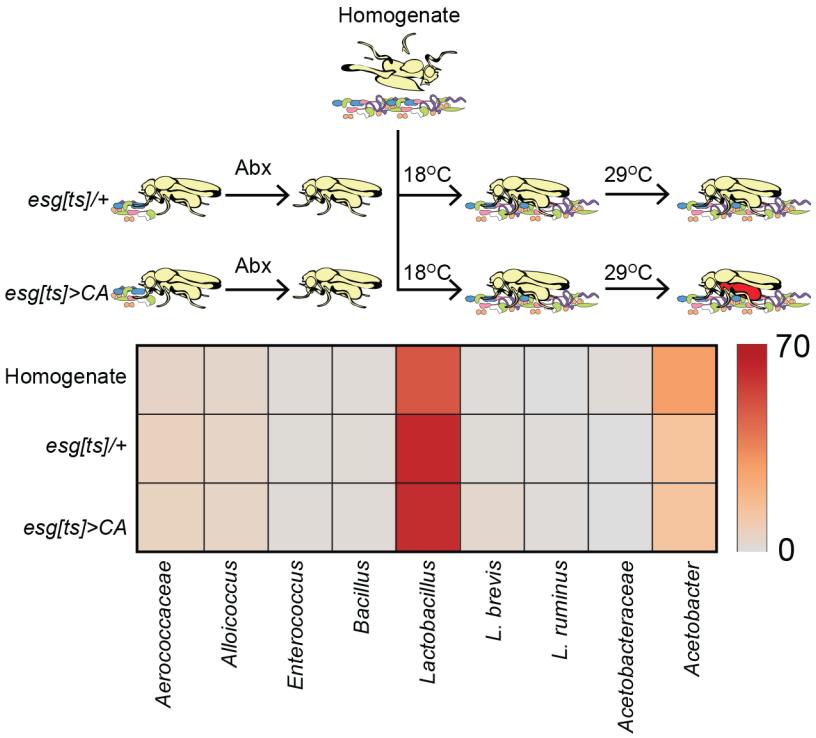

192 Kruskall-Wallis test: H=0.1 df=2 P=0.9512

193

194 **Figure 4. Induced expression of ImdCA in intestinal progenitor cells does not have a substantial**

195 **impact on gut microbiome composition.** Heat map analysis of microbial original taxonomic unit

196 representation in dissected midguts of the indicated genotypes. All flies were raised under

197 identical conditions, and fed the same homogenate at the same time. Kruskall-Wallis test results

198 for degree of difference between the different samples.

199

200

201 *Constitutive IMD Pathway Activation Causes Dysplasia in Intestinal Progenitor Cells.*

202 In contrast to the minimal effects on bacterial microbiome composition, we noticed that
203 ImdCA affected expression of regulators of intestinal homeostasis. This included elements of
204 Wnt, Ras, Insulin, JNK and JAK/STAT pathways (Figure 5B). This led us to ask if ImdCA impacts
205 intestinal morphology. To address this question, we examined the posterior midguts of two,
206 eleven and twenty-six day old *esg*^{ts}*>CA* and control *esg*^{ts} flies. In these lines, the *esg*^{ts} regulatory
207 system marks all progenitors with GFP. We found that acute activation of the IMD pathway had
208 no effect on midgut architecture. The posterior midguts of two-day old *esg*^{ts} and *esg*^{ts}*>CA* flies
209 raised at 29°C were essentially indistinguishable (Figure 6A). In both cases, anti-Armadillo (beta-
210 catenin ortholog) immunofluorescence showed a regular arrangement of large, polyploid ECs,
211 that were interspersed with small, Prospero positive EE cells. Likewise, the posterior midguts of
212 both genotypes contained regularly spaced nuclei and evenly distributed GFP positive progenitor
213 cells (Figure 6A).

214

A

GENE	ISC	EB	EC	EE	VM
PGRP-LC	6.13	7.96	6.432	1.365	4.263
IMD	3.534	4.249	7.41	7.473	7.55
IAP2	10.171	16.595	13.329	15.8	12.292
DREDD	1.684	1.712	1.694	1.506	1.747
FADD	6.649	11.527	11.19	11.997	3.282
TAB2	2.413	2.222	4.253	6.007	3.373
TAK1	4.121	7.004	7.89	5.929	9.594
KEY	19.999	52.248	42.098	19.39	39.636
IRD5	0.97	0.765	1.076	0.782	0.906
REL	40.397	52.647	39.985	14.71	42.481

Expression value (rpkm) per cell type

B

Gene	Function	Fold Change (*esgCA* V *esg*)	ANOVA p-value
MESK2	Ras signaling	-2.15	0.000349
gfzg	Ras signaling	-1.84	0.000116
cdi	Ras signaling	1.59	0.001404
Plzf	Ras signaling	-1.66	0.025787
CG42684	Ras signaling	2	0.000475
dock	Insulin signaling	-1.56	0.016287
srl	Insulin signaling	1.59	0.012109
sug	Insulin signaling	-1.68	0.025726
egr	JNK signaling	1.68	0.001723
Traf4	JNK signaling	1.64	0.000984
nmo	Wnt signaling	-1.98	0.000068
ebd1	Wnt signaling	1.53	0.008942
sfl	Wnt signaling	1.96	0.002488
Prosap	Wnt signaling	-1.53	0.002859
SOCS36E	JAK/STAT	-1.84	0.038907

C

Gene	Function	Fold Change (*esgCA* V *esg*)	ANOVA p-value
mahe	Notch signaling	1.54	0.000941
neur	Notch signaling	-1.55	0.001857
Nle	Notch signaling	1.63	0.010107
Rala	Notch signaling	2.07	0.000403
stv	Lateral Inhibition	-1.61	0.005874
Cam	Lateral Inhibition	-1.54	0.007552
CG13827	Lateral Inhibition	-1.74	0.003491
CG16713	Lateral Inhibition	-1.86	0.000181
CG5953	Lateral Inhibition	-1.81	0.002646
CG7631	Lateral Inhibition	-2.19	0.000129
CG9194	Lateral Inhibition	-1.89	0.001998

215

216 **Figure 5. A:** Expression of IMD pathway components in intestinal cell types. Expression data taken
217 from (Dutta et al., 2015). **B-C:** Homeostatic regulators (B) and Notch pathway components (C)
218 that were dysregulated in *esg*^{ts}*>CA* flies relative to *esg*^{ts} flies.
219
220 By day 11, the posterior midguts of *esg*^{ts}*>CA* flies appeared moderately dysplastic relative to
221 *esg*^{ts} flies. By 26 days, the posterior midguts of control *esg*^{ts} flies displayed classical hallmarks of
222 age-dependent dysplasia such as a disorganized epithelium, uneven arrangements of nuclei, and
223 irregular patterns of GFP expression (Figure 6A). We noticed that midgut architecture was further
224 disrupted in 26 day-old *esg*^{ts}*>CA* flies. In this case, we detected a near complete breakdown of
225 epithelial organization (Figure 6A), an increase in cell density, and an increase in GFP positive
226 cells. The hyperplastic phenotype of 26 day old *esg*^{ts}*>CA* flies is not a consequence of accelerated
227 physiological aging, as *esg*^{ts} and *esg*^{ts}*>CA* flies have indistinguishable lifespans (Figure 6I).
228 Given the hyperplasia and altered expression of homeostatic regulators in older *esg*^{ts}*>CA*
229 flies, we reasoned that ImdCA affects proliferation rates in intestinal progenitor cells. To test this
230 hypothesis, we used anti-phosphorylated histone H3 immunofluorescence to count mitotic cells
231 in the intestines of fourteen and twenty-four day-old *esg*^{ts} and *esg*^{ts}*>CA* files. At both ages, we
232 detected a significant increase in mitotic events in *esg*^{ts}*>CA* intestines relative to age-matched
233 *esg*^{ts} controls (Figure 6D). These data show that persistent expression of ImdCA in adult midgut
234 progenitor cells disrupts expression of homeostatic regulators, increases cell proliferation, and
235 promotes tissue hyperplasia.
236

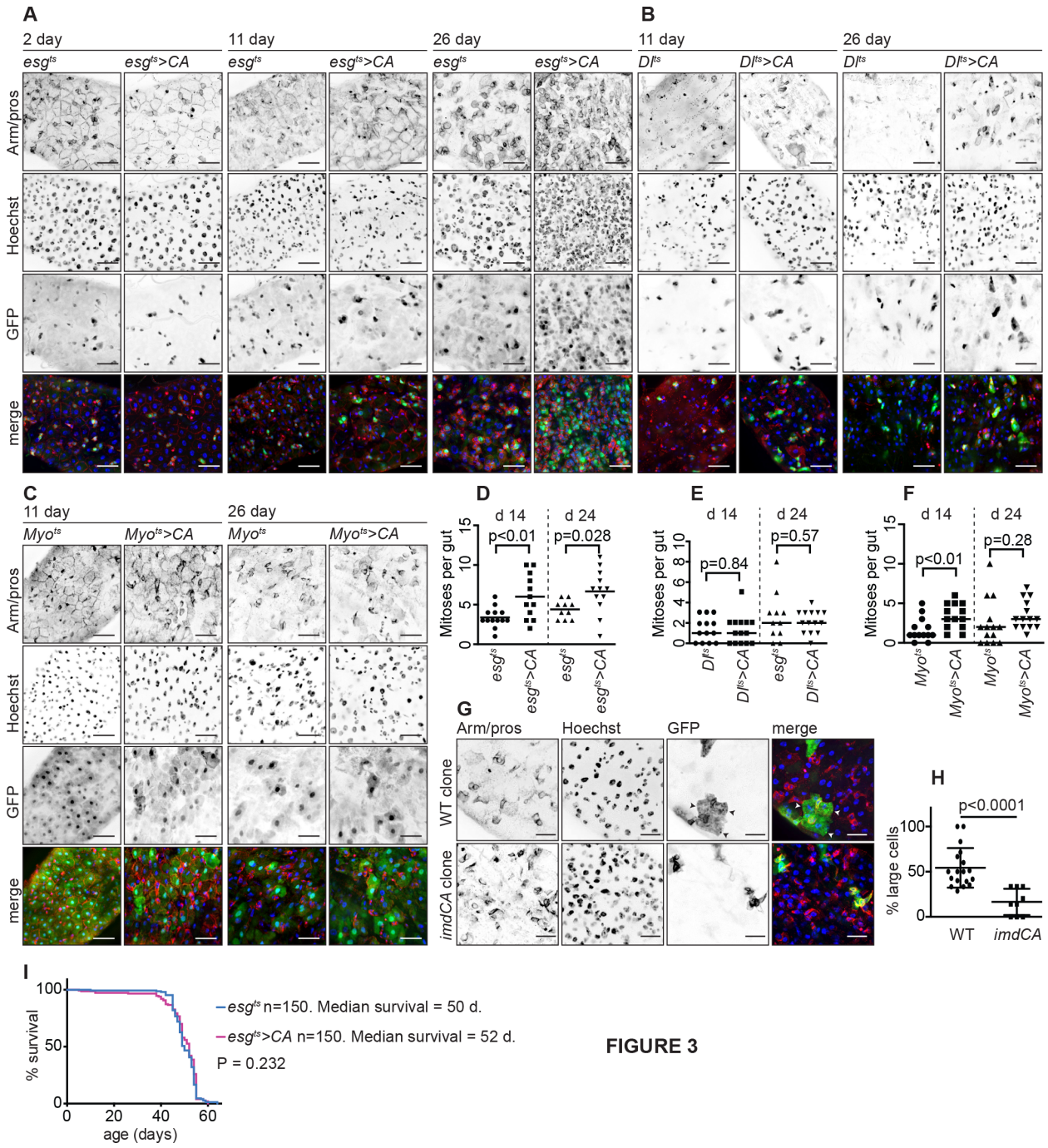

FIGURE 3

Figure 6. Intestinal hyperplasia in the posterior midguts of *esg^{ts}>CA* flies. (A-C) Immunofluorescence imaging of the posterior midguts of *esg^{ts}>CA* and *esg^{ts}* flies (A); *Dl^{ts}>CA* and *Dl^{ts}* flies (B); and *myo1a^{ts}>CA* and *myo1a^{ts}* flies (C) raised at 29°C for 2, 11 or 26 days as indicated.

242 Each midgut was stained with Armadillo (to indicate cell borders), and Prospero to reveal
243 enteroendocrine cells; Hoechst to reveal nuclei; and GFP was visualized to reveal progenitor cells
244 (A), stem cells (B) and enterocytes (C). All images were taken at 40X magnification and scale bars
245 show 25 µm. **(D-F)** Number of mitotic cells in the intestines of flies of the indicated genotypes
246 raised at 29°C for 14 and 24 days. **G:** Visualization of mitotic clones in wild type flies (upper row)
247 or mitotic clones that express *imdCA* (lower row). All images were taken at 60X magnification and
248 scale bars show 15 µm **H:** Percentage of large, enterocyte-type cells in wild type clones and *imdCA*
249 positive clones. Comparisons were performed with a student's t test. **(I)** Survival curves for 150
250 esg^{ts}>*CA* and 150 esg^{ts} flies raised at 29°C.
251
252 We did not see a similar phenotype when we used a Dl^{ts} line (*UASGFP* ; *DlGAL4*, $GAL80^{ts}$) to
253 express ImdCA in GFP-marked stem cells. In this case, midgut morphology and proliferation rates
254 were indistinguishable between Dl^{ts}>*CA* and control Dl^{ts}/+ flies at all times (Figure 6B and E).
255 Expression of ImdCA in GFP-marked intestinal enterocytes with the $Myo1A^{ts}$ (*UASGFP* ;
256 *Myo1aGAL4*, $GAL80^{ts}$) line led to a mild increase in midgut proliferation at d14 that did not persist
257 at later times (Figure 6C and F). Thus, expression of ImdCA in progenitor cells led to a marked
258 hyperplasia throught the posterior midgut. As the Dl^{ts} line, fails to induce hyperplasia our data
259 suggest that activation of IMD either in progenitor pairs, or enteroblasts alone leads to midgut
260 hyperplasia.
261
262
263

264 *Persistent IMD Signals Disrupt Notch Activity.*

265 Among homeostatic regulators, ImdCA had a pronounced effect on expression of Notch
266 pathway components (Figure 5B). This observation matches an earlier report of deregulated
267 expression of Notch pathway genes in *imd* mutant flies (Broderick et al., 2014), and raises the
268 possibility that the IMD pathway influences Notch activity in the adult. To test if ImdCA affects
269 progenitor cell differentiation, we used MARCM analysis to identify individual mitoses and
270 subsequent differentiation events in adult posterior midguts. As expected, mitotic clones in
271 conventional flies contained a mix of smaller cells (most likely progenitors and EE), and larger,
272 polyploid ECs (Figure 6G). In contrast, we rarely detected large, polyploid cells in mitotic clones
273 that express ImdCA. Instead, ImdCA clones typically contained aggregates of small cells (Figure
274 6G). These observations suggest that persistent expression of ImdCA in progenitor cells affects
275 the differentiation of EBs into ECs.

276 To directly test the possibility that ImdCA disturbs EB differentiation, we determined the
277 percentage of EE cells in the intestines of twenty-four days old *esg*^{ts} and *esg*^{ts}*>CA* flies. As
278 expected, the posterior midguts of *esg*^{ts}*>CA* flies contained greater numbers of cells per area
279 than those observed in age-matched, control *esg*^{ts} flies (Figure 7A-C). However, we also found
280 that a significantly greater percentage of midgut cells expressed the EE marker Prospero in
281 *esg*^{ts}*>CA* than in *esg*^{ts} midguts (Figure 7A, B, D). These data show that persistent expression of
282 ImdCA disrupts the developmental trajectory of progenitor cells, and leads to the differentiation
283 of supernumerary EE.

284

285

286 *IMD Pathway Activity Promotes the Development of Notch-Mediated Intestinal Tumors.*

287 As bacterial challenges enhance *Notch*-deficient tumor formation (Apidianakis et al., 2009,
288 Jiang et al., 2009), and ImdCA influences *Notch*-dependent events, we asked what effects
289 persistent immune signals have on models of *Notch*-deficient tumorigenesis in the posterior
290 midgut. To answer this question, we used a validated, inducible RNAi line that blocks *Notch*
291 signaling in GFP-marked adult progenitors ($esg^{ts}>N^{RNAi}$). As anticipated, the posterior midguts of
292 $esg^{ts}>N^{RNAi}$ flies contained GFP-positive tumors composed of small, irregularly spaced nuclei
293 within eight days of Notch depletion (Figure 7E, F). Many tumors also contained patches of
294 Prospero-positive enteroendocrine cells (Figure 7F). The ability of $esg^{ts}>N^{RNAi}$ to promote
295 tumorigenesis appears to require extrinsic inputs from the microbiome, as removal of the gut
296 microbiome greatly reduced the incidence of tumor formation in $esg^{ts}>N^{RNAi}$ posterior midguts
297 (Figure 7G, H). This observation matches an earlier report that growth of *Notch* loss-of-function
298 tumors requires stress-induced mitogenic cues (Patel et al., 2015).

299

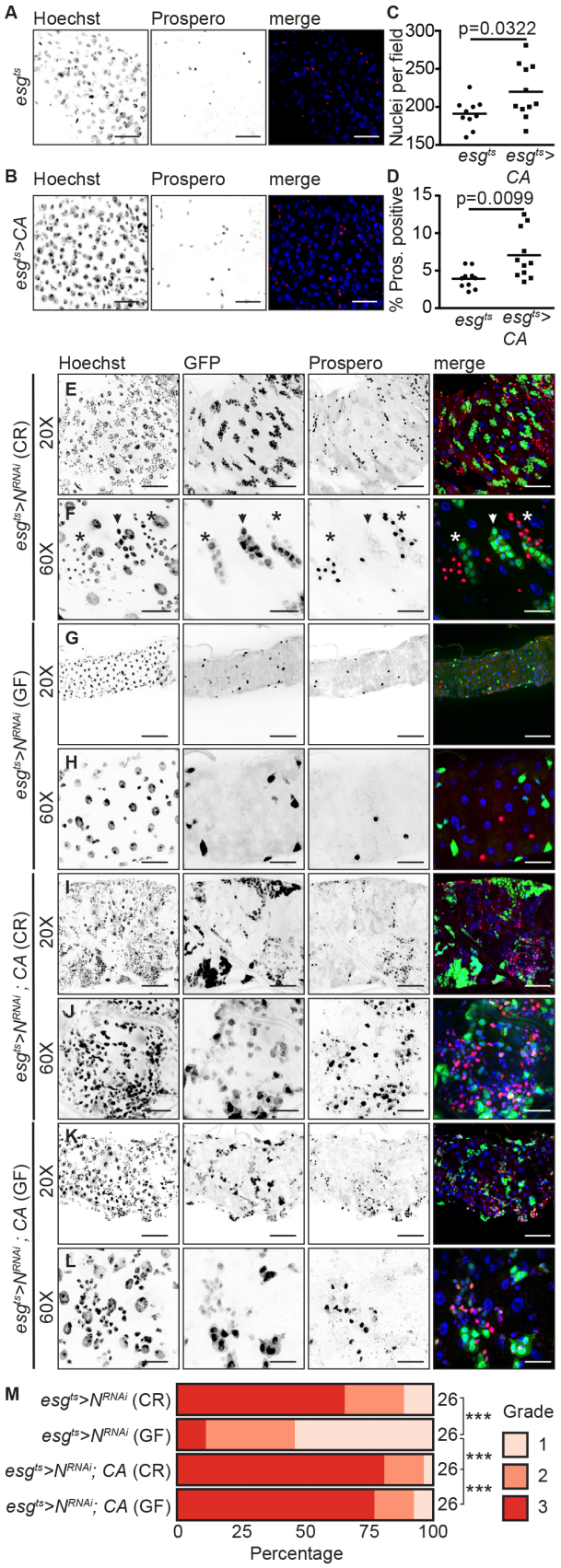
A
Hoechst
Prospero
merge
esg^ts
B
esg^ts>CA
C
Nuclei per field
p=0.0322
esg^ts
esg^ts> CA
D
% Pros. positive
p=0.0099
GFP
E
F
G
H
I
J
K
L
20X
60X
esg^ts>N^RNAi (CR)
esg^ts>N^RNAi (GF)
esg^ts>N^RNAi ; CA (CR)
esg^ts>N^RNAi ; CA (GF)
M
Grade
1
2
3
Percentage

300

301 **Figure 7. ImdCA promotes tumorigenesis in Notch-deficient progenitor cells. (A-B)** Midguts of
302 20d old *esg*^{ts} (A) and *esg*^{ts}*>CA* (B) flies stained for DNA and Prospero as indicated. Images were
303 false-colored and merged with DNA in blue and Prospero in red. Images were taken at 40X
304 magnification and scale bars show 25 µm. **C:** Automated quantification of total nuclei in a given
305 field for flies of both genotypes. **D:** Total percentage of Prospero positive cells in the same fields.
306 For C and D comparisons were performed with a student's t test. **E-L:** Visualization of
307 tumorigenesis in 8d old *esg*^{ts}*>N*^{RNAi} and *esg*^{ts}*>N*^{RNAi}; *CA* flies. Posterior midguts were stained for
308 Prospero and DNA in conventionally-reared *esg*^{ts}*>N*^{RNAi}; flies (E-F); germ-free *esg*^{ts}*>N*^{RNAi} flies (G-
309 H); conventionally-reared *esg*^{ts}*>N*^{RNAi}; *CA* flies (I-J); and germ-free *esg*^{ts}*>N*^{RNAi}; *CA* flies (K-L). In all
310 cases, progenitor cells were visualized through the expression of GFP. Scale bars show 50µm for
311 20X magnification images, and 15µm for 60X images. A representative grade 2 tumor is indicated
312 with an arrowhead in F, and representative grade 3 tumors are shown with an asterisk. **M:** Tumor
313 scoring in the posterior midguts of 8d old flies with the indicated genotypes and culture
314 conditions (n=26) for each condition. Tumor grade was compared between individual treatments
315 using one-way ANOVA, with Tukey's correction. *** indicates P<0.0001.
316
317 Whereas elimination of the microbiome blocked tumorigenesis in *esg*^{ts}*>N*^{RNAi} flies, co-
318 expression of ImdCA with *N*^{RNAi} (*esg*^{ts}*>N*^{RNAi}; *CA*) exacerbated the formation of midgut tumors.
319 We invariably detected large patches of GFP and Prospero positive cells in *esg*^{ts}*>N*^{RNAi}; *CA*
320 posterior midguts, with few large cells characteristic of mature ECs (Figure 7 I, J). To determine if
321 ImdCA alone provides sufficient stress signals to promote tumorigenesis in this *Notch* loss-of-
322 function model, we examined the posterior midguts of germ-free *esg*^{ts}*>N*^{RNAi}; *CA* flies. We found

323 that nearly all midguts of germ-free *esg*^{ts}*>CA, N*^{RNAi} flies had accumulations of small, GFP-positive
324 cells, large patches of Prospero positive tumors, and few large polyploid ECs (Figure 7K, L). To
325 quantify the effects of microbiome elimination on tumorigenesis, we developed a grading system
326 for tumor scale in the posterior midgut. We defined tumor-free intestines as Grade 1 (e.g. Figure
327 7G, H), tumors that only contained GFP-positive clusters of cells as Grade 2 (Figure 7F, asterisks),
328 and tumors that contained clusters of GFP-positive and Prospero-positive cells as Grade 3 (Figure
329 7F, arrowhead). We used this system to quantify tumor grade in 26 intestines from each
330 experimental condition. This scale confirmed a significant reduction of tumor formation in germ-
331 free *esg*^{ts}*>N*^{RNAi} flies (Figure 7M), and a significant increase of tumorigenesis in germ-free
332 *esg*^{ts}*>N*^{RNA} *; CA* flies (Figure 7M).This phenotype is remarkably similar to one described earlier for
333 bacterial infection of *esg*^{ts}*>N*^{RNAi} flies (Apidianakis et al., 2009, Jiang et al., 2009), and shows that
334 immune signaling in progenitor cells alone is sufficient to promote *Notch*-dependent tumor
335 growth in adult midguts.
336

337 **DISCUSSION**

338

339 Animal genomes encode evolutionarily conserved systems that mitigate the threats posed by
340 potentially harmful microbes. For example, homeostatic resistance systems clear invading
341 microbes, while tolerance mechanisms limit the damage caused by invaders (Medzhitov et al.,
342 2012, Schneider and Ayres, 2008) . In this study, we used the genetically accessible fruit fly to
343 activate immune responses exclusively in intestinal progenitor cells. We focused on progenitors,
344 as they are immune-competent, but comparatively understudied from the perspective of IMD.
345 We showed that persistent immune activity causes intestinal hyperplasia, disrupts progenitor cell
346 differentiation, and fuels Notch-dependent tumorigenesis. These phenotypes occur without
347 significant shift in bacterial populations, consistent with altered disease tolerance in the host.
348 Our studies match reports of relationships between the microbiota, inflammation and colorectal
349 cancer (Belkaid and Hand, 2014, Irrazabal et al., 2014), and uncover a novel requirement for
350 regulated innate immune activity in the overall maintenance of progenitor cell homeostasis in
351 the fly.

352 In *Drosophila*, several homeostatic devices control progenitor cell proliferation and
353 differentiation, often in response to bacterial products (Amcheslavsky et al., 2009, Buchon et al.,
354 2009, Jiang et al., 2009). For example, flies raised in the absence of a microbiome undergo fewer
355 mitoses in the midgut (Buchon et al., 2009). In addition, flies raised in a germ-free environment
356 have atypical numbers of prospero-positive EE cells, a lower density of ECs, and deregulated
357 expression of Notch pathway components (Broderick et al., 2014). It is unclear how much of this
358 response requires an intact IMD pathway, although recent transcriptional work established that

359 mutations of the IMD pathway impact numerous aspects of intestinal transcription (Broderick et
360 al., 2014, Erkosar et al., 2014), including Notch pathway components (Broderick et al., 2014). Our
361 work shows that expression of ImdCA in progenitor cells alone recapitulates key features of those
362 host responses to gut microbes. For example, of the 253 genes differentially expressed in the
363 intestines of conventionally-reared flies compared to germ-free flies, 87 are affected by
364 expression of ImdCA. Additionally, expression of ImdCA in progenitor cells boosts intestinal
365 mitoses, affects EE cell differentiation, and increases EC density. Combined, these data implicate
366 the IMD pathway as a novel regulator of progenitor cell proliferation.

367 As the microbiome induces progenitor cell proliferation, we initially assumed that ImdCA-
368 dependent hyperplasia was the result of a dysbiosis in the gut caused by immune activity.
369 However, expression of ImdCA does not influence microbiome composition. These data raise the
370 possibility that common intestinal microbes are insensitive to IMD activity in the gut, or that
371 elevated immune signaling activates counter-defenses in commensal populations, thereby
372 allowing persistence of commensal bacteria. This matches experimental data that commensal
373 bacteria effectively overcome host innate defenses in other models. For example, many gut-
374 resident *Firmicutes* and *Bacteroidetes* are not susceptible to antimicrobial peptides (Cullen et al.,
375 2015), and NOD deficient mice do not display dysbiosis (Robertson et al., 2013, Shanahan et al.,
376 2014). These observations lead us propose that constitutive activation of IMD acts directly on the
377 host to induces intestinal hyperplasia. Although out data are more consistent with IMD acting in
378 enteroblasts to promote hyperplasia, additional experiments are required to rule out a need for
379 IMD activity in progenitor pairs. We believe that the ability of ImdCA to promote Notch-
380 dependent tumors is of particular significance in the context of aging. As flies age, clones of *Notch*

381 mutant cells spontaneously develop in the intestine (Siudeja et al., 2015), and host immune
382 activity gradually rises (Buchon et al., 2009). Our data suggest that age-dependent increases in
383 immune activity may contribute to the formation, or growth, of Notch-dependent tumors in the
384 fly. Indeed, we found that elimination of the microbiome was sufficient to arrest the appearance
385 of Notch-dependent tumors.

386 The role of Notch in tumorigenesis is not restricted to flies. Several studies established clear
387 links between deregulated Notch activity and carcinogenesis in vertebrates (Rizzo et al., 2008,
388 Shih Ie and Wang, 2007). Colorectal cancer lines and adenocarcinomas express elevated levels of
389 Notch1 and Notch 2 (Fre et al., 2009, Guilmeau et al., 2010, Reedijk et al., 2008, Sikandar et al.,
390 2010). In addition, manipulations of Notch pathway activity modify tumorigenesis in mouse
391 models of colorectal cancer (Fre et al., 2009, Rodilla et al., 2009). The mechanisms that activate
392 Notch in colon cancer are unclear at present. Given the broad conservation of immune activity
393 and Notch signaling in the guts of flies and mammals, our work raises the possibility that chronic
394 inflammation is a long-term activator of Notch-dependent tumorigenesis. The data in this study
395 present a simple model to precisely describe the relationships between intestinal immune
396 activity and the formation of Notch-dependent tumors.

397

398 **EXPERIMENTAL PROCEDURES**

399

400 ***Drosophila* husbandry.**

401 All flies were raised on standard corn meal medium (Nutri-Fly Bloomington Formulation, Genesse
402 Scientific). Germ-free husbandry conditions are described in the Supplementary methods. For
403 16S deep-sequencing, we raised freshly eclosed virgin females flies on antibiotic medium for 5 d
404 at 18°C, then switched to sterile antibiotic-free food for 1 d. Next, flies were fed a homogenate
405 prepared from w^{1118} flies for 16 h. Afterwards, flies were raised on sterile antibiotic-free food at
406 18°C for 7 d. Flies were moved to 29°C for another 7 days, and 10 guts/sample were dissected.
407 We extracted microbial DNA with the UltraClean® Microbial DNA Isolation Kit (MoBio
408 Laboratories Inc.), and amplified 16S DNA with Platinum® PFX Taq (Invitrogen), followed by
409 purification with the QIAquick® PCR Purification Kit (Qiagen). Concentration was measured on
410 the Qubit® 2.0 (Invitrogen) and 1 ng was used for library prep. Libraries were prepared using the
411 Nextera XT DNA Library Preparation Kit (Illumina). We purified libraries using Ampure Beads
412 (Qiagen) and quantified using the Qubit® 2.0 (Invitrogen) and Bioanalyzer 2100 (Agilent). Pooled
413 libraries were loaded on the Miseq (illumina) using the MiSeq Reagent Kit v3 (600-cycle) for
414 sequencing. 16S sequences were assembled using DNASTAR Navigator, and annotated with the
415 greengenes database. For infection studies, freshly eclosed flies were raised for 5 d at 18°C, then
416 switched to 29°C for 2 d. 24 h before infection 100 µl of a *V. cholerae* C6706 glycerol stock was
417 spread on LB agar plates and grown at 29°C. Flies were starved for 2 h before infection. The
418 bacterial lawn was scraped from the plate and mixed into LB broth, then diluted to an OD600 of
419 0.125, flies were fed 3ml bacterial supernatant on a cotton plug, and dead flies counted every 2-

420 4 h. To generate mitotic clones, flies were raised at 18°C for 5-6 d, incubated at 37°C for 2 h, and
421 raised for an additional 8-10 days at 25°C.
422
423 **Cell culture and molecular biology.**
424 The Imd expression construct used in this study has been described elsewhere (Guntermann and
425 Foley, 2011). To generate ImdCA, we used pENTR/D-TOPO ImdCA forward and reverse primers
426 (supplemental material) to amplify a truncated Imd. We then cloned truncated Imd with into the
427 pENTR/D-TOPO plasmid according to manufacturer's instructions (Invitrogen). We recombined
428 TOPO-ImdCA with pAWM, or pTW (LR recombination, Invitrogen) to generate ImdCA-6myc and
429 UAS-ImdCA expression plasmids. Transgenic lines were generated by Bestgene Inc.
430 Immunoprecipitation and Western blot protocols have been described elsewhere (Guntermann
431 and Foley, 2011). For immunoprecipitation assays, we incubated cell lysate with mouse anti-HA
432 (Sigma, 1:500) at 4°C overnight, added protein G-Sepharose beads and incubated for an
433 additional hour at 4°C. Beads were pelleted by centrifugation at 300 X g for 30 s and washed in
434 lysis buffer three times. After discarding the supernatant, beads were re-suspended in 2X sample
435 buffer, and analyzed by Western blot.
436
437 **Gene expression analysis.**
438 We used TRIZOL to prepare RNA from dissected adult intestines (Guntermann and Foley, 2011).
439 Microarray studies were performed in triplicate on virgin flies that we raised on regular or
440 antibiotic-treated food food for 10-11 days at 29°C. We then shifted flies to 29°C for another 2
441 days, after which guts were dissected for RNA extraction (5 females and 5 males per sample). We

442 used 100 ng purified RNA to make labeled cRNA for microarrays using the GeneChip® 3' IVT Plus
443 Reagent Kit (Affymetrix), then fragmented cRNA and then hybridized to the
444 GeneChip®Drosophila Genome 2.0 Array (Affymetrix). Preliminary analysis was done in the
445 Transciptome Analysis Console (TAC) software (Affymetrix). We analyzed gene expression data
446 using FlyMINE (Lyne et al., 2007) and Panther (Thomas et al., 2003). Array data has been
447 submitted to the NCBI GEO database (accession ID: GSE89445). For qPCR studies, we prepared 1
448 µg cDNA from purified RNA using qScript cDNA Supermix (Quanta Biosciences, Inc.) and then
449 performed qPCR using the PerfeCTa® SYBR®Green FastMix (Quanta Biosciences, Inc.). All qPCR
450 studies were performed in triplicate and relative expression values were calculated using delta
451 delta Ct calculations. In each case, expression levels were normalized to *actin*.
452
453 **Immunofluorescence.**
454 The immunofluorescence protocol used in this study has been described elsewhere (Petkau et
455 al., 2014). All immunofluorescence images were prepared from the posterior midgut of adult flies
456 at a distance of approximately 50 µM from the hindgut transition. To quantify phospho-histone
457 H3 positive cells, guts were visualized under the microscope and scanned from posterior midgut
458 (hindgut transition area) to anterior midgut (crop). To quantify Prospero positive cells, we used
459 the Columbus software to identify the percentage of Hoechst positive cells that were also
460 prospero positive. 3-D reconstructions were created with Volocity® 6.3 (Perkin Elmer).
461

462 **Germ-Free Adult Fly Husbandry.**

463 Larval growth and development is supported by commensal microbes. As our primary goal was to examine
464 the effects of immune signaling in an adult model of intestinal tumorigenesis, we were concerned that
465 elimination of the larval microbiome would influence gut development, and possibly confound
466 interpretation of our data. For that reason, we chose to raise larvae under conventional conditions, and
467 exclusively remove the bacterial microbiome from adults. To generate germ-free animals, we raised
468 freshly eclosed adult flies on sterile food containing an antibiotic cocktail (100 µg/ml Ampicillin, 100 µg/ml
469 Neomycin, 100 µg/ml Metronidazole and 50 µg/ml Vancomycin). This protocol allowed us to raise larvae
470 in the presence of a conventional microbiome, and restrict our examination of germ-free phenotypes to
471 the adult life stage. We confirmed bacterial elimination by plating fly homogenates on agar plates
472 permissive for the growth of *Lactobacilli* and *Actetobacter*.

473

474 **Primers used in this study.**

Gene	Forward Primer	Reverse Primer
pENTR/D-TOPO ImdCA	CACCGCAGCTCCCGTGGACGACAACG	CTAGCTGTTTGTCTTGCGC
16S	AGAGTTTGATCCTGGCTCAG	GGCTACCTTGTTACGACTT
att	AGTCACAACTGGCGGAAC	TGTTGAATAAATTGGCATGG
dpt	ACCGCAGTACCCACTCAATC	ACTTTCCAGCTCGGTTCTGA
actin	TGCCTCATCGCCGACATAA	CACGTCACCAGGGCGTAAT
totM	ACCGGAACATCGACAGCC	CCAGAATCCGCCTTGTGC
pirk	AGAGCACGAGCAGGGTAAATC	TGTTGTTCTCAATGCGGTACTC

pgrp-sc1	AAGCGATCGTCAACTATT	GAGAGCCACTTTGGAAACCA
cec	TGTAAGCTAGTTTATTTCTATGG	GATGAGCCTTTAATGTCC

475

476 **Antibodies used in this study.**

Antigen	Use	Source
Tubulin.	Western blot (1:1000)	Developmental Studies Hybridoma Bank E7
cMyc	Western blot (1:5000)	Sigma
HA	Western blot (1:4000)	Sigma
JNK	Western blot (1:4000)	Santa Cruz sc-571
Armadillo	Immunofluorescence (1:100)	Developmental Studies Hybridoma Bank N2 7A1
Prospero	Immunofluorescence (1:100)	Developmental Studies Hybridoma Bank MR1A
phospho- H3(Ser10)	Immunofluorescence (1:1000)	Millipore
pgrp-sc1	AAGCGATCGTCAACTATT	GAGAGCCACTTTGGAAACCA
cec	TGTAAGCTAGTTTATTTCTATGG	GATGAGCCTTTAATGTCC

477

478 **Fly Genotypes**

479 Clonal analysis was performed with flies of the following genotypes: *hsFLP, UASGFP/X* ;
480 *tubGAL80, neoFRT40A/neoFRT40A* ; *tubGAL4/+* (wild-type), and *hsFLP, UASGFP/X* ; *tubGAL80,*
481 *neoFRT40A/neoFRT40A* ; *tubGAL4/UASimdCA* (ImdCA positive clones).

482 **AUTHOR CONTRIBUTIONS**

483 K.P., M.F., S.G., and E.F. conceived and designed experiments; K.P., M.F., and S.G. performed the
484 experiments; K.P., M.F., and E.F performed data analysis and wrote the paper.

485

486 **ACKNOWLEDGEMENTS**

487 Transgenic flies were provided by Bruce Edgar (*esg*^{ts}), Bruno Lemaitre (*dredd*), the Bloomington
488 *Drosophila* stock Center (*cgGAL4* and *GAL80*^{ts}), and the Vienna *Drosophila* Resource Center
489 (N^{RNAi}). The research was funded by a grant from the Canadian Institutes of Health Research to
490 EF (MOP 77746). We acknowledge the microscopy support from Dr. Stephen Ogg and the Faculty
491 of Medicine and Dentistry core imaging service, the Cell Imaging Centre, University of Alberta.
492 Microarrays were processed at the Alberta Transplant Applied Genomics Center. We are grateful
493 to Juan Jovel for bioinformatics advice.

494

495 **REFERENCES**

496 AMCHESLAVSKY, A., JIANG, J. & IP, Y. T. 2009. Tissue damage-induced intestinal stem cell
497 division in Drosophila. *Cell Stem Cell,* 4**,** 49-61.
498 APIDIANAKIS, Y., PITSOULI, C., PERRIMON, N. & RAHME, L. 2009. Synergy between bacterial
499 infection and genetic predisposition in intestinal dysplasia. *Proc Natl Acad Sci U S A,* 106**,**
500 20883-8.
501 BELKAID, Y. & HAND, T. W. 2014. Role of the microbiota in immunity and inflammation. *Cell,*
502 157**,** 121-41.
503 BITEAU, B. & JASPER, H. 2011. EGF signaling regulates the proliferation of intestinal stem cells in
504 Drosophila. *Development,* 138**,** 1045-55.
505 BRODERICK, N. A., BUCHON, N. & LEMAITRE, B. 2014. Microbiota-induced changes in drosophila
506 melanogaster host gene expression and gut morphology. *MBio,* 5**,** e01117-14.
507 BUCHON, N., BRODERICK, N. A., CHAKRABARTI, S. & LEMAITRE, B. 2009. Invasive and
508 indigenous microbiota impact intestinal stem cell activity through multiple pathways in
509 Drosophila. *Genes Dev,* 23**,** 2333-44.
510 BUCHON, N., BRODERICK, N. A. & LEMAITRE, B. 2013. Gut homeostasis in a microbial world:
511 insights from Drosophila melanogaster. *Nat Rev Microbiol,* 11**,** 615-26.
512 BUCHON, N., SILVERMAN, N. & CHERRY, S. 2014. Immunity in Drosophila melanogaster--from
513 microbial recognition to whole-organism physiology. *Nat Rev Immunol,* 14**,** 796-810.
514 CHO, I. & BLASER, M. J. 2012. The human microbiome: at the interface of health and disease.
515 *Nat Rev Genet,* 13**,** 260-70.
516 CROSNIER, C., VARGESSON, N., GSCHMEISSNER, S., ARIZA-MCNAUGHTON, L., MORRISON, A. &
517 LEWIS, J. 2005. Delta-Notch signalling controls commitment to a secretory fate in the
518 zebrafish intestine. *Development,* 132**,** 1093-104.
519 CULLEN, T. W., SCHOFIELD, W. B., BARRY, N. A., PUTNAM, E. E., RUNDELL, E. A., TRENT, M. S.,
520 DEGNAN, P. H., BOOTH, C. J., YU, H. & GOODMAN, A. L. 2015. Gut microbiota.
521 Antimicrobial peptide resistance mediates resilience of prominent gut commensals
522 during inflammation. *Science,* 347**,** 170-5.
523 DUSHAY, M. S., ASLING, B. & HULTMARK, D. 1996. Origins of immunity: Relish, a compound Rel-
524 like gene in the antibacterial defense of Drosophila. *Proc Natl Acad Sci U S A,* 93**,** 10343-
525 7.
526 DUTTA, D., DOBSON, A. J., HOUTZ, P. L., GLASSER, C., REVAH, J., KORZELIUS, J., PATEL, P. H.,
527 EDGAR, B. A. & BUCHON, N. 2015. Regional Cell-Specific Transcriptome Mapping Reveals
528 Regulatory Complexity in the Adult Drosophila Midgut. *Cell Rep,* 12**,** 346-58.
529 ERKOSAR, B., DEFAYE, A., BOZONNET, N., PUTHIER, D., ROYET, J. & LEULIER, F. 2014. Drosophila
530 microbiota modulates host metabolic gene expression via IMD/NF-kappaB signaling.
531 *PLoS One,* 9**,** e94729.
532 FINK, C., HOFFMANN, J., KNOP, M., LI, Y., ISERMANN, K. & ROEDER, T. 2016. Intestinal FoxO
533 signaling is required to survive oral infection in Drosophila. *Mucosal Immunol,* 9**,** 927-36.
534 FRE, S., HUYGHE, M., MOURIKIS, P., ROBINE, S., LOUVARD, D. & ARTAVANIS-TSAKONAS, S. 2005.
535 Notch signals control the fate of immature progenitor cells in the intestine. *Nature,* 435**,**
536 964-8.

537 FRE, S., PALLAVI, S. K., HUYGHE, M., LAE, M., JANSSEN, K. P., ROBINE, S., ARTAVANIS-TSAKONAS,
538 S. & LOUVARD, D. 2009. Notch and Wnt signals cooperatively control cell proliferation
539 and tumorigenesis in the intestine. *Proc Natl Acad Sci U S A,* 106**,** 6309-14.
540 GUILMEAU, S., FLANDEZ, M., MARIADASON, J. M. & AUGENLICHT, L. H. 2010. Heterogeneity of
541 Jagged1 expression in human and mouse intestinal tumors: implications for targeting
542 Notch signaling. *Oncogene,* 29**,** 992-1002.
543 GUNTERMANN, S. & FOLEY, E. 2011. The protein Dredd is an essential component of the c-Jun
544 N-terminal kinase pathway in the Drosophila immune response. *J Biol Chem,* 286**,**
545 30284-94.
546 GUO, Z. & OHLSTEIN, B. 2015. Stem cell regulation. Bidirectional Notch signaling regulates
547 Drosophila intestinal stem cell multipotency. *Science,* 350.
548 HONDA, K. & LITTMAN, D. R. 2016. The microbiota in adaptive immune homeostasis and
549 disease. *Nature,* 535**,** 75-84.
550 HOOPER, L. V., LITTMAN, D. R. & MACPHERSON, A. J. 2012. Interactions between the
551 microbiota and the immune system. *Science,* 336**,** 1268-73.
552 IRRAZABAL, T., BELCHEVA, A., GIRARDIN, S. E., MARTIN, A. & PHILPOTT, D. J. 2014. The
553 multifaceted role of the intestinal microbiota in colon cancer. *Mol Cell,* 54**,** 309-20.
554 JIANG, H. & EDGAR, B. A. 2012. Intestinal stem cell function in Drosophila and mice. *Curr Opin*
555 *Genet Dev,* 22**,** 354-60.
556 JIANG, H., PATEL, P. H., KOHLMAIER, A., GRENLEY, M. O., MCEWEN, D. G. & EDGAR, B. A. 2009.
557 Cytokine/Jak/Stat signaling mediates regeneration and homeostasis in the Drosophila
558 midgut. *Cell,* 137**,** 1343-55.
559 KAZANJIAN, A. & SHROYER, N. F. 2011. NOTCH Signaling and ATOH1 in Colorectal Cancers. *Curr*
560 *Colorectal Cancer Rep,* 7**,** 121-127.
561 LEMAITRE, B. & MIGUEL-ALIAGA, I. 2013. The digestive tract of Drosophila melanogaster. *Annu*
562 *Rev Genet,* 47**,** 377-404.
563 LHOCINE, N., RIBEIRO, P. S., BUCHON, N., WEPF, A., WILSON, R., TENEV, T., LEMAITRE, B.,
564 GSTAIGER, M., MEIER, P. & LEULIER, F. 2008. PIMS modulates immune tolerance by
565 negatively regulating Drosophila innate immune signaling. *Cell Host Microbe,* 4**,** 147-58.
566 LYNE, R., SMITH, R., RUTHERFORD, K., WAKELING, M., VARLEY, A., GUILLIER, F., JANSSENS, H., JI,
567 W., MCLAREN, P., NORTH, P., RANA, D., RILEY, T., SULLIVAN, J., WATKINS, X.,
568 WOODBRIDGE, M., LILLEY, K., RUSSELL, S., ASHBURNER, M., MIZUGUCHI, K. & MICKLEM,
569 G. 2007. FlyMine: an integrated database for Drosophila and Anopheles genomics.
570 *Genome Biol,* 8**,** R129.
571 MARIANES, A. & SPRADLING, A. C. 2013. Physiological and stem cell compartmentalization
572 within the Drosophila midgut. *Elife,* 2**,** e00886.
573 MEDZHITOV, R., SCHNEIDER, D. S. & SOARES, M. P. 2012. Disease tolerance as a defense
574 strategy. *Science,* 335**,** 936-41.
575 MICCHELLI, C. A. & PERRIMON, N. 2006. Evidence that stem cells reside in the adult Drosophila
576 midgut epithelium. *Nature,* 439**,** 475-9.
577 OHLSTEIN, B. & SPRADLING, A. 2006. The adult Drosophila posterior midgut is maintained by
578 pluripotent stem cells. *Nature,* 439**,** 470-4.
579 OHLSTEIN, B. & SPRADLING, A. 2007. Multipotent Drosophila intestinal stem cells specify
580 daughter cell fates by differential notch signaling. *Science,* 315**,** 988-92.

581 PAQUETTE, N., BROEMER, M., AGGARWAL, K., CHEN, L., HUSSON, M., ERTURK-HASDEMIR, D.,
582 REICHHART, J. M., MEIER, P. & SILVERMAN, N. 2010. Caspase-mediated cleavage, IAP
583 binding, and ubiquitination: linking three mechanisms crucial for Drosophila NF-kappaB
584 signaling. *Mol Cell,* 37**,** 172-82.
585 PATEL, P. H., DUTTA, D. & EDGAR, B. A. 2015. Niche appropriation by Drosophila intestinal stem
586 cell tumours. *Nat Cell Biol,* 17**,** 1182-92.
587 PATEL, P. H. & EDGAR, B. A. 2014. Tissue design: how Drosophila tumors remodel their
588 neighborhood. *Semin Cell Dev Biol,* 28**,** 86-95.
589 PEIGNON, G., DURAND, A., CACHEUX, W., AYRAULT, O., TERRIS, B., LAURENT-PUIG, P.,
590 SHROYER, N. F., VAN SEUNINGEN, I., HONJO, T., PERRET, C. & ROMAGNOLO, B. 2011.
591 Complex interplay between beta-catenin signalling and Notch effectors in intestinal
592 tumorigenesis. *Gut,* 60**,** 166-76.
593 PERDIGOTO, C. N., SCHWEISGUTH, F. & BARDIN, A. J. 2011. Distinct levels of Notch activity for
594 commitment and terminal differentiation of stem cells in the adult fly intestine.
595 *Development,* 138**,** 4585-95.
596 PETKAU, K., PARSONS, B. D., DUGGAL, A. & FOLEY, E. 2014. A deregulated intestinal cell cycle
597 program disrupts tissue homeostasis without affecting longevity in Drosophila. *J Biol*
598 *Chem,* 289**,** 28719-29.
599 REEDIJK, M., ODORCIC, S., ZHANG, H., CHETTY, R., TENNERT, C., DICKSON, B. C., LOCKWOOD, G.,
600 GALLINGER, S. & EGAN, S. E. 2008. Activation of Notch signaling in human colon
601 adenocarcinoma. *Int J Oncol,* 33**,** 1223-9.
602 RIZZO, P., OSIPO, C., FOREMAN, K., GOLDE, T., OSBORNE, B. & MIELE, L. 2008. Rational targeting
603 of Notch signaling in cancer. *Oncogene,* 27**,** 5124-31.
604 ROBERTSON, S. J., ZHOU, J. Y., GEDDES, K., RUBINO, S. J., CHO, J. H., GIRARDIN, S. E. &
605 PHILPOTT, D. J. 2013. Nod1 and Nod2 signaling does not alter the composition of
606 intestinal bacterial communities at homeostasis. *Gut Microbes,* 4**,** 222-31.
607 RODILLA, V., VILLANUEVA, A., OBRADOR-HEVIA, A., ROBERT-MORENO, A., FERNANDEZ-
608 MAJADA, V., GRILLI, A., LOPEZ-BIGAS, N., BELLORA, N., ALBA, M. M., TORRES, F.,
609 DUNACH, M., SANJUAN, X., GONZALEZ, S., GRIDLEY, T., CAPELLA, G., BIGAS, A. &
610 ESPINOSA, L. 2009. Jagged1 is the pathological link between Wnt and Notch pathways in
611 colorectal cancer. *Proc Natl Acad Sci U S A,* 106**,** 6315-20.
612 SCHNEIDER, D. S. & AYRES, J. S. 2008. Two ways to survive infection: what resistance and
613 tolerance can teach us about treating infectious diseases. *Nat Rev Immunol,* 8**,** 889-95.
614 SHANAHAN, M. T., CARROLL, I. M., GROSSNIKLAUS, E., WHITE, A., VON FURSTENBERG, R. J.,
615 BARNER, R., FODOR, A. A., HENNING, S. J., SARTOR, R. B. & GULATI, A. S. 2014. Mouse
616 Paneth cell antimicrobial function is independent of Nod2. *Gut,* 63**,** 903-10.
617 SHIH IE, M. & WANG, T. L. 2007. Notch signaling, gamma-secretase inhibitors, and cancer
618 therapy. *Cancer Res,* 67**,** 1879-82.
619 SIKANDAR, S. S., PATE, K. T., ANDERSON, S., DIZON, D., EDWARDS, R. A., WATERMAN, M. L. &
620 LIPKIN, S. M. 2010. NOTCH signaling is required for formation and self-renewal of tumor-
621 initiating cells and for repression of secretory cell differentiation in colon cancer. *Cancer*
622 *Res,* 70**,** 1469-78.
623 SIUDEJA, K., NASSARI, S., GERVAIS, L., SKORSKI, P., LAMEIRAS, S., STOLFA, D., ZANDE, M.,
624 BERNARD, V., RIO FRIO, T. & BARDIN, A. J. 2015. Frequent Somatic Mutation in Adult

625 Intestinal Stem Cells Drives Neoplasia and Genetic Mosaicism during Aging. *Cell Stem*
626 *Cell,* 17**,** 663-74.
627 STANGER, B. Z., DATAR, R., MURTAUGH, L. C. & MELTON, D. A. 2005. Direct regulation of
628 intestinal fate by Notch. *Proc Natl Acad Sci U S A,* 102**,** 12443-8.
629 TAKASHIMA, S., ADAMS, K. L., ORTIZ, P. A., YING, C. T., MORIDZADEH, R., YOUNOSSI-
630 HARTENSTEIN, A. & HARTENSTEIN, V. 2011. Development of the Drosophila entero-
631 endocrine lineage and its specification by the Notch signaling pathway. *Dev Biol,* 353**,**
632 161-72.
633 THOMAS, P. D., CAMPBELL, M. J., KEJARIWAL, A., MI, H., KARLAK, B., DAVERMAN, R., DIEMER,
634 K., MURUGANUJAN, A. & NARECHANIA, A. 2003. PANTHER: a library of protein families
635 and subfamilies indexed by function. *Genome Res,* 13**,** 2129-41.
636 VAN ES, J. H., VAN GIJN, M. E., RICCIO, O., VAN DEN BORN, M., VOOIJS, M., BEGTHEL, H.,
637 COZIJNSEN, M., ROBINE, S., WINTON, D. J., RADTKE, F. & CLEVERS, H. 2005.
638 Notch/gamma-secretase inhibition turns proliferative cells in intestinal crypts and
639 adenomas into goblet cells. *Nature,* 435**,** 959-63.
640 WLODARSKA, M., KOSTIC, A. D. & XAVIER, R. J. 2015. An integrative view of microbiome-host
641 interactions in inflammatory bowel diseases. *Cell Host Microbe,* 17**,** 577-91.
642